Adhesion and Permeability of Polyimide–Clay Nanocomposite Films for Protective Coatings

Orasa Khayankarn,[1] Rathanawan Magaraphan,[1] Johannes W. Schwank[2]

[1]*Petroleum and Petrochemical College, Chulalongkorn University, Bangkok 10330, Thailand*
[2]*Department of Chemical Engineering, University of Michigan, Ann Arbor, Michigan, 48109-2136*

Received 21 June 2002; accepted 12 November 2002

ABSTRACT: A polyimide (PI)–clay nanocomposite was prepared from a solution of poly(amic acid), a precursor of 2,2-bis[4-(3,4-dicarboxyphenoxy)phenyl]propane dianhydride and *p*-phenylenediamine, and dodecylamine–montmorillonite. Fourier transform infrared spectroscopy, thermogravimetric analysis, X-ray diffraction, and atomic absorption spectroscopy were used to verify the incorporation of the modifying agents into the clay structure and the intercalation of the modified clay into the PI matrix. Both PI and PI–clay films were subsequently prepared by solution casting. The gas permeability, resistivity, and adhesion properties were determined. In the case of gas permeability, only a 3 wt % addition of clay reduced oxygen permeability to less than half that of unfilled PI. Furthermore, this hybrid showed an improvement in electrical resistivity because of the prevention of electrical tree growth by clay particles. More importantly, adhesion between the films and silicon increased with increasing clay content. © 2003 Wiley Periodicals, Inc. J Appl Polym Sci 89: 2875–2881, 2003

Key words: adhesion; gas permeation; polyimides; clay; nanocomposites

INTRODUCTION

Polyimide (PI) is well known as a high-temperature engineering polymer. Compared to most other organic or polymeric materials, PI exhibits an exceptional combination of thermal stability (>500°C), mechanical toughness, and chemical resistance. In addition, it has excellent dielectric properties. Because of its high degree of ductility and inherently low thermal expansion coefficient (CTE), PI can be readily implemented into a variety of microelectronic applications.[1–6] Thin-film applications on large silicon substrates can be achieved. In the past decade, the development of micromachined silicon-based devices, such as solid-state gas sensors, has grown rapidly because of the lower manufacturing cost, lower energy consumption, and faster response. These sensors can be used to monitor the purity of microelectronic processing gases and environmental and automotive exhaust gases. Chemical vapor deposition (CVD) is a commonly used technique for the deposition of electrically conductive thin films on gas sensor devices. It is important to protect the backside of the sensor device during CVD to avoid shorting out the electrodes and electrical contacts on the sensor chip. PI is an appropriate protective material for the backside of the sensor because it can fulfill almost all of the specific requirements, which include a high thermal stability, a low CTE, a high electrical insulation, good adhesion, and a low gas permeability.[3–5]

It is difficult for pure PI to meet all of the coating requirements. However, it was interesting to investigate how the PI properties could be improved by the addition of an inorganic filler to produce a nanocomposite material. Composites that exhibit a change in composition and structure over a nanometer length, *nanocomposites*, have been shown over the last 10 years to afford remarkable property enhancements relative to conventionally scaled composites.[7] Layered silicates dispersed as a reinforcing phase in an engineering polymer matrix are one of the most important forms of such hybrid organic–inorganic nanocomposites. Montmorillonite (MMT) is one of the clay minerals; its is about 2000 Å in length and 10 Å in thickness. It has a sandwich-type structure called a *philo-silicate* with one octahedral Al_2O_3 sheet between two tetrahedral SiO_2 sheets. To make an organophilic clay intercalated with an ammonium salt of dodecylamine (Do), it is necessary to use a clay that swells in water.[2] These PI–clay nanocomposites showed low CTEs and good barrier properties for both water vapor and helium and oxygen gasses due to the long silicate sheets of MMT (2180 Å). These properties were further improved when longer clay platens, such as those in synthetic mica (12,300 Å), were used.[1,2] Moreover, the nanocomposites with a clay loading lower than 5 wt % showed good dispersion for the organophilic clay with a large expansion of silicate layers, good mechan-

Correspondence to: R. Magaraphan (krathana@chula.ac.th).
Contract grant sponsor: New Faculty Development, Chulalongkorn University.

ical properties, a high thermal stability, and solubility in polar aprotonic solvents. The properties were especially superior when a long alkyl amine, such as hexadecylamine, was used as a modifying agent (better than a bulky substituted amine).[8,9] At a high loading of organophilic clay (e.g., 10 wt %), Lan et al.[10] found that intercalated-type PI–clay nanocomposites were obtained via the contraction of silicate layers.

In our previous work, thermogravimetric analysis (TGA) and transmission electron microscopy (TEM) results showed that PI–clay films with 1–6 wt % clay had an optimum content of clay; these films exhibited appropriate properties for microelectronic coating: low CTE, low water absorption, and high mechanical and dielectric strengths.[11] However, the protective film also requires a low gas permeability, good adhesion to a silicon substrates, and appropriate electrical insulation (resistivity = 10^5–10^{18} Ω cm). In this study, the oxygen permeability, adhesion, and electrical resistivity of nanocomposites were investigated as functions of clay content, coating thickness, and use temperature.

EXPERIMENTAL

Materials

Pyralin BPDA–PDA poly(amic acid) in *N*-methyl-2-pyrrolidone (NMP) solution (solid content = 10.5%) was provided by DuPont Co. Sodium MMT (Kunipia-F) with a cation exchange capacity of 119 meg/100 g was supplied by Kunimine Industrial Co., Ltd. (Japan). NMP, used as a solvent, was purchased from Merck. Do from Fluka was used as a modifying agent. Hydrochloric acid (HCl; 36 wt %) from Univar was used without further purification. An adhesion promoter (VM-651), an aminosilane-based adhesion promoter [γ-amino propyltriethoxysilane (γ-APS)], which had to be diluted to 0.5% before application, was a product of HD Microsystems, an enterprise of Hitachi Chemical and DuPont Electronics.

Characterization and property measurements

Wide-angle X-ray diffraction (WAXD) was used to determine the basal spacing in the nanocomposite materials and was performed at room temperature with a Rigaku model D/MAX 2000 diffractometer with a Cu Kα radiation source, which was operated at 40 kV and 30 mA. A DuPont 2950 thermogravimetric analyzer was used to carry out the thermal characterizations of the nanocomposites. A Varian SpectrAA-300 atomic absorption spectrometer at a wavelength of 589.0 nm was used to determine the percentage of sodium ions exchanged from the clay. The percentage of sodium ions exchanged from the sodium MMT in the process of the preparation of the organophilic clay was determined by atomic absorption spectroscopy (AAS) with an air–acetylene flame. The percentage of Na^+ exchanged was calculated by eq. (1):

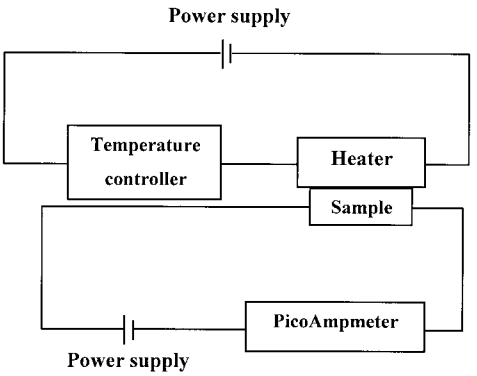

Figure 1 Diagram of the resistivity measurement unit.

$$\%\ Na^+\ \text{exchange} = \frac{\text{Amount of actual } Na^+}{\text{Amount of theoretical } Na^+} \times 100\% \quad (1)$$

Fourier transform infrared spectroscopy (FTIR) spectra were recorded on a Bruker spectrometer (Equinox 55) in the wavenumber range 4000–400 cm^{-1}. A Brugger gas permeability tester was used for the estimation of the steady-state rate of transmission of gas through plastics in the form of film, sheeting, and laminates, according to ASTM D 1434-82. The measuring gas was fed into the tester cell at a flow rate of 100 cm^3/min at 25°C. The gas permeability (G), in units of $cm^3/(m^2$ day bar), was calculated from eqs. (2) and (3) (with appropriate machine factors):

$$G = \frac{7.76 \times 10^{10} \times V}{78.5K \times 29N} \quad cm^3/(m^2\ \text{day bar}) \quad (2)$$

where V is the volume of the evacuation chamber, K is the absolute temperature (in degrees Kelvin), and N is the slope of the plot between the temperature and the reading scale corresponding to the chamber pressure. When the evacuation chamber volume is 0.4370 cm^3, this expression simplifies to

$$G = \frac{1.49 \times 10^7}{KN} \quad cm^3/(m^2\ \text{day bar}) \quad (3)$$

The resistivity measurement unit shown in Figure 1 was used to measure the resistivity of films at different temperatures from 50 to 350°C. The resistivity (ρ) was calculated by eq. (4):

$$\rho = \frac{Vyz}{Ix} \quad (\Omega\ \text{cm}) \quad (4)$$

where V is the voltage, I is the current, x is the length of the sample, y is the width of the sample, and z is the thickness of the sample. An Instron universal testing machine (model 4206) at a gauge length (initial grip separation) of 50 mm and with an applied 5-kN load cell was used to determine the shear strength of the interface between the PI and the PI–clay nanocomposite thin films and silicon wafers, according to the method described in the ASTM D 1002 lap shear test. We prepared the samples by first treating a silicon wafer with the VM-651 adhesion promotor and then coating it with PI or PI–clay film. Subsequently, the silicon wafer coated with PI or PI–clay was glued to steel plates on both sides with epoxy glue. Then, the loading was applied immediately to pull the specimen at a crosshead speed of 50 mm/min. The load at failure was recorded and expressed in shear strength in units of N/mm^2 (MPa) with eq. (5):

$$\text{Shear strength} = \frac{F}{A} \quad (N/mm^2) \tag{5}$$

where F is the applied load at failure and A is the adhesion area.

Preparation of the organophilic clay filler

In a 500-mL beaker, 4.41 g of Do, 2.4 mL of concentrated hydrochloric acid, and 100 mL of distilled water were placed. This solution was heated to 80°C. In 200 mL of water, 10 g of clay was dispersed at 80°C for 1 h. The dispersion of MMT was added to the solution of the ammonium salt of Do, and this mixture was stirred vigorously at 80°C for 1 h. A white precipitate was isolated by filtration, placed in a 500-mL beaker with 200 mL of hot water, and stirred for 1 h. This process was repeated twice to remove the residue of the ammonium salt of Do. The organophilic clay was

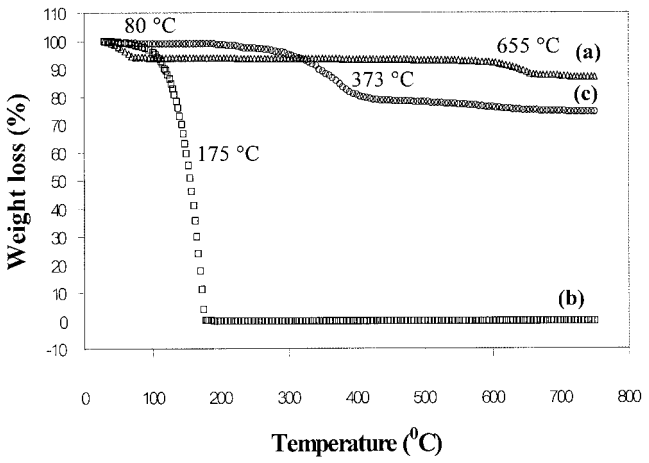

Figure 2 TGA thermograms of (a) sodium MMT, (b) Do, and (c) Do–MMT.

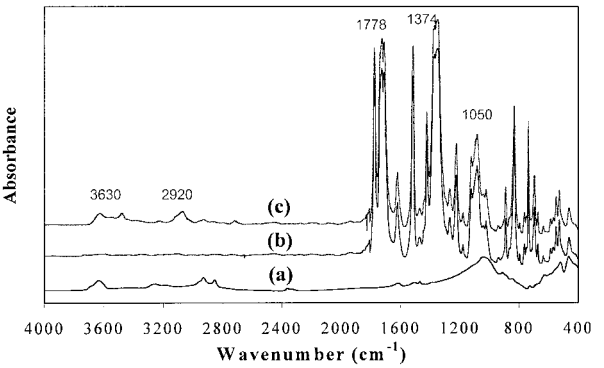

Figure 3 FTIR spectra of (a) Do–MMT, (b) PI, and (c) PI–MMT.

then collected and dried. Consequently, the organophilic clay filler was characterized to verify the structure and composition with FTIR, WAXD, TGA, and AAS.

Preparation of the PI–clay nanocomposite thin films

A mixture of 0.15 g of organophilic clay and 5 g of NMP solvent was stirred vigorously at 90°C for 3 h, yielding 3.5 wt % clay in the NMP solvent. Pyralin BPDA–PDA poly(amic acid) solution was diluted with the NMP solvent and was then mixed with the stock solution of clay dispersed in NMP and stirred vigorously at 30°C for 3 h, yielding a poly(amic acid)–clay mixture solution.

A drop of ordinary poly(amic acid) and poly(amic acid)–clay solution was cast on a glass substrate (onto a silicon wafer for the adhesion test) by a hand-coating technique. The wet film was dried at 150°C for 3 h and finally imidized at 300°C for 2 h at heating a rate of 2°C/min in a nitrogen atmosphere oven. Then, the film was cooled down to 30°C at a rate of 5°C/min. Finally, the films were characterized to inspect their compositions and characteristics with FTIR, WAXD, and TGA.

RESULTS AND DISCUSSION

From the results, 10 g of sodium MMT, which has an ion exchange capacity of 119 meq/100 g, presented 250 mg of sodium ions. Consequently, the percentage of sodium ions exchanged was equal to 91.34%. TGA. The thermograms for sodium MMT, Do, and Do–MMT are shown in Figure 2.

The onset of sodium MMT decomposition was found at about 655°C. There was a slight weight loss at 80°C due to the evaporation of absorbed water in the clay. For Do, the sample showed a dramatic decomposition at a temperature of 175°C, as shown in Figure 2(b). The mean decomposition temperature of Do–

TABLE I
FTIR Absorption Band Assignments of Do–MMT

Frequency (cm^{-1})	Assignment
3630	—OH stretching
3440	—OH stretching (dimers)
3320	N—H stretching of the primary amine
2920	C—H stretching of the —CH_2— aliphatic chain
2850	C—H stretching of CH_3
1600	Symmetric N—H bending
1460	C—H bending of the —CH_2— aliphatic chain
1370	C—H bending of CH_3
1050	Si—O stretching
1010	C—N stretching in the aliphatic amine
720	N—H out-of-plane bending
520	Al—O stretching
460	Si—O bending

MMT was between the decomposition temperatures of sodium MMT and Do at 373°C. This was an indication that dodecylammonium ions reacted with the clay and that this ammonium salt possessed quite a high thermal stability.[10,11] Furthermore, the thermogram of the Do–MMT showed an absence of evaporation of absorbed water in the sample at 80°C.

Characterization of the PI–clay nanocomposite thin films

The IR spectra illustrated in Figure 3 and listed in Table I are for Do–MMT, PI, and PI–MMT. Clearly, the spectra of the composites exhibited the presence of characteristic absorption due to both the organic and inorganic groups. The absorption bands at 3630, 2920, and 1050 and those between 600–400 cm^{-1} could be associated with —OH stretching of the lattice water, C—H stretching, Si—O stretching, and Al—O stretching, respectively, in Do–MMT. For the PI in Figure 3(b), one can clearly see bands at 1778 and 1726 cm^{-1}, which are characteristic of carbonyl group (C═O) stretching in imide groups, and the band at 1374 cm^{-1}, which is characteristic of C—N stretching in imide groups.[12] Figure 3(c) is for the PI–MMT nanocomposite film, which demonstrated both the characteristic

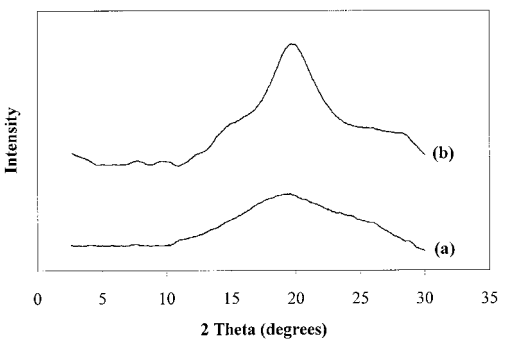

Figure 4 WAXD patterns of (a) PI and (b) PI–MMT.

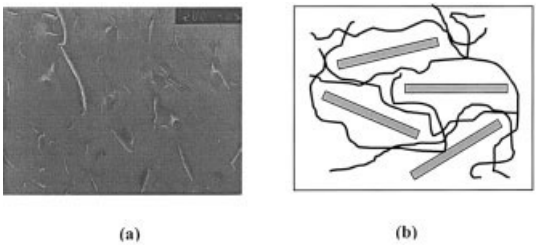

Figure 5 (a) TEM micrograph of a PI–clay nanocomposite film (3 wt % clay) and (b) a schematic of the exfoliated nanocomposite.

peaks of Do–MMT and PI. The mean degradation temperature of Do–MMT was higher than the curing temperature of 300°C, so at this temperature, the onium ion was stable, and its characteristic peaks could still be seen in the FTIR spectrum of the nanocomposite.[10,11]

Figure 4 shows the X-ray diffraction curves of PI and PI–MMT (3 wt % clay). In the case of PI–MMT (3 wt % clay), the curve showed no peak, indicating that the peak corresponding to the basal spacing disappeared. This suggested that the organophilic clay in the nanocomposite material dispersed homogeneously into the PI matrix.[7] Therefore, the PI–clay nanocomposite at 3 wt % could be classified as an exfoliated nanocomposite, as shown by the WAXD and TEM results in Figure 5. The broad band in the region between 2θ = 12 and 30° suggested that the films contained amorphous regions or partially ordered structures. The TEM micrograph illustrates that the exfoliated long silicate layers were distributed randomly in the matrix.

The TGA curves of the PI and PI–clay nanocomposites are shown in Figure 6. The decomposition temperatures of PI and PI–clay were 585 and 625°C, respectively. The onset of PI matrix decomposition in the nanocomposite was found to move to a higher temperature than that of pure PI, indicating enhancement of the thermal stability of the composite. This resulted from hydrophobic interaction between the PI

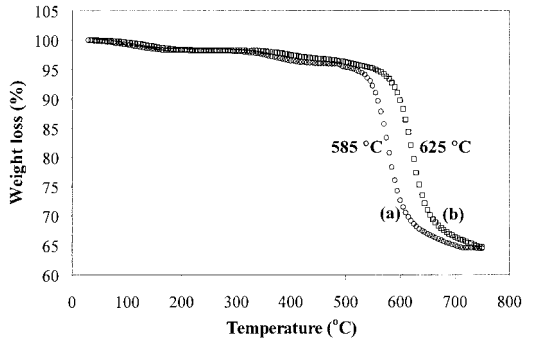

Figure 6 TGA thermograms of the (a) PI and (b) PI–clay films.

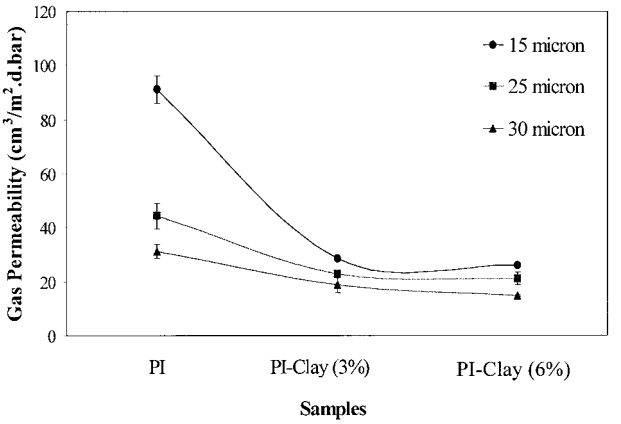

Figure 7 MMT content and film-thickness dependence of the O_2 gas permeability of the PI–clay hybrids.

chain and the alumino-silicate layer of the filler. An additional amount of thermal energy was probably needed to destroy this specific interaction, so the inorganic filler could delay the thermal degradation of the polymeric material.

Property measurements

Gas permeability

As a protective coating for gas sensors, a polymer should have a low level of gas permeability to avoid any uncontrolled changes in the sensitivity of the gas sensor. Figure 7 shows the O_2 gas permeability of PI, PI–clay (3%), and PI–clay (6%) with various thicknesses of 15, 25, and 35 μm. The PI–clay nanocomposite was superior in its gas barrier properties to ordinary PI. Furthermore, the content dependence of MMT on the O_2 gas permeability was also investigated. The results showed that the higher the content of clay was, the lower the O_2 gas permeability was. Only a 3 wt % addition of MMT brought the gas permeability to a value of less than half of that of pure PI. This big decrease in the gas permeability was explained by the increase in the diffusion path of the gas.[1,9–11,13] As shown by TEM, MMT was disposed parallel to the film surface. Therefore, the total path of

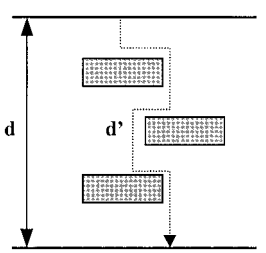

Figure 8 Model for the path of a diffusing gas through the PI–clay hybrid (d = film thickness and d' = tortuosity path of a diffusing gas).

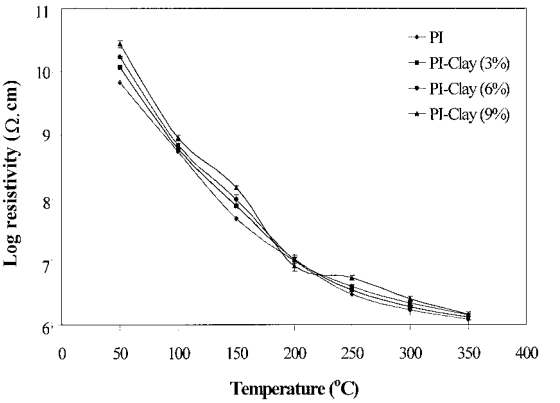

Figure 9 Resistivity measurement of the PI–clay hybrid.

the diffusing gas could increase markedly. Moreover, oxygen gas permeability decreased with increasing thickness, as was found with increasing the clay content. Figure 8 shows a conceptual picture of the path of a diffusing gas through the PI–clay hybrid. Increasing the thickness led to increasing the tortuosity of the diffusing pathway.[2]

Resistivity

As a protective coating for microelectronic gas sensor applications, resistivity is of functional significance.[14] Figure 9 shows the resistivity of PI and PI–clay hybrids with various clay contents. A higher loading of clay contents raised the resistivity of the films in the temperature range 50–350°C. This evidence could be explained by the prevention of the intermolecular charge transfer of the PI chain.[14] Dense packing is necessary for the formation of the ordered structures required for intermolecular charge transfer. Therefore, in the PI–clay hybrids, the clay acted as a hindrance, which reduced the possibility for the polymer chain to form well-packed donor/acceptor pairs. Moreover, the electrical treeing could be inhibited by the presence of certain finely divided inorganic fillers.[15] The increased resistivity was possibly caused by the inhibition of electrical treeing by clay particles.

The dependence of the temperature on resistivity is also shown in Figure 9. As the temperature increased, the electrical resistivity of the films decreased remarkably. At the highest temperature, 350°C, the resistivity dropped from the order of 10^{10} Ω cm to 10^6 Ω cm, which was still in the range of resistivity for an insu-

TABLE II
Classification of Materials Based on Resistivity

ρ (Ω cm)	Class
0–10^3	Conductor
10^3–10^7	Partial conductor or semiconductor
10^5–10^{18} and higher	Insulator

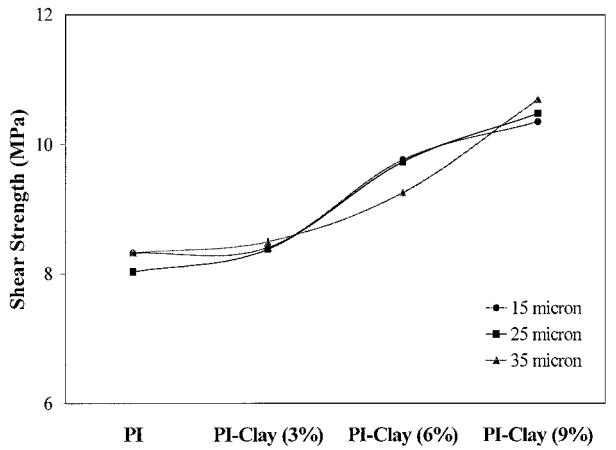

Figure 10 Shear strength between the PI–clay hybrid and a silicon wafer.

lator, as shown in Table II. The decline of resistivity can be described by the energy band concept.[15] At any finite temperature, some electrons in the ground state can be thermally excited across the energy gap into the empty orbital in the conduction band, leaving behind unoccupied positive holes in the valence band. Because the electrons in the bottom of the conduction band and the positive hole in the top of the valence band are in the same molecular orbital that extends throughout the entire material, both can contribute to the conduction process, leading to a reduction in resistivity.

Adhesion

In the microelectronics field, γ-APS has been used for adhesion improvement between PI and silicon wafers. This is due to the chemical interaction of silane with the silicon substrate (SiO_2) surface and with the PI matrix. The γ-APS molecule bonds to the substrate via covalent bond formation and forms an interpenetrating network with the polymer matrix.[14] The covalent bond has a high bond energy (70–800 kJ/mol) and is a desired interfacial interaction, leading to a reliable bond.

Figure 10 shows the shear strength between the PI–clay hybrid and the silicon wafer. A higher clay content brought the shear strength to a value greater than that of the original unfilled PI. Because γ-APS was applied between the PI–clay and the silicon wafer, the ionic interaction of the ammonium group (NH_3^+) at the γ-APS chain end could occur with negative charges normally generated on the surface of the silicate layer of the clay, as shown in Figure 11. Because the ionic bond (electrostatic interaction) also had a high bond energy (160–600 kJ/mol) relative to that of the covalent bond, the higher clay content could bring about an increment of shear strength. Moreover, thickness had no effect on the adhesion between the films and the silicon substrate because a prerequisite for chemical interaction is the closeness of the active sites across the interface. Interaction between active sites become unimportant when the distance between the reacting groups is in excess of 0.5 nm.[14]

With zoom stereo microscopy, the detached surfaces (of both sides), obtained after pulling by the Instron universal testing machine, were smooth. This suggests that an adhesive failure, not cohesive failure, occurred at the interface between the thin film and the silicon substrate.

CONCLUSIONS

A PI–clay nanocomposite where MMT was dispersed at the molecular level was prepared with a poly(amic acid) precursor of BPDA–PDA and an organophilic

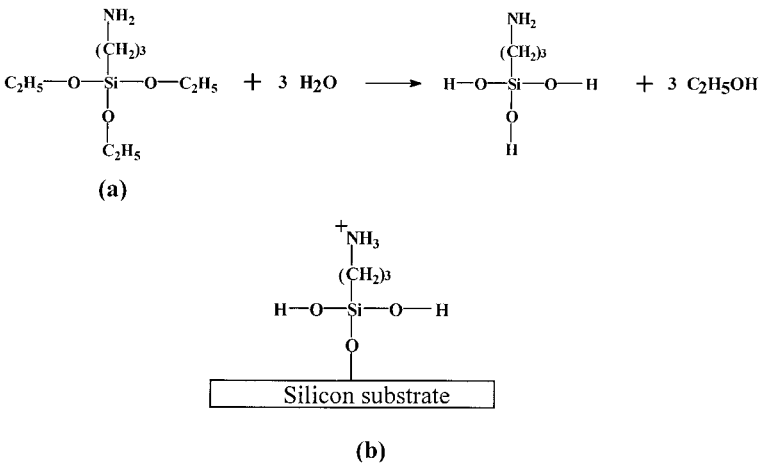

Figure 11 (a) Chemical structure of γ-APS and the hydrolysis reaction, (b) its bonds with the substrate and the PI matrix, and (c) the ionic bonds between γ-APS and the silicate layer.

modified MMT. As seen from WAXD patterns of the nanocomposite films, this hybrid had a special structure exhibiting exfoliated silicate layers with homogeneous dispersion. These results suggest that the PI–clay hybrid could be classified as an exfoliated nanocomposite.

Because of this special structure, the PI–clay nanocomposite showed a marked improvement in thermal properties, gas permeability, resistivity, and adhesion properties. TGA results showed a thermal stability improvement by as much as 40°C above that of untreated polymer. In the case of gas permeability, only a 3 wt % addition of clay brought the permeability of O_2 to a value less than half of that of ordinary unfilled PI. Furthermore, this hybrid showed an improvement in resistivity due to the prevention of electrical tree growth by clay particles and matrix-hindering electron jumps. A higher loading of clay raised the resistivity of the films in the temperature range 50–350°C. More important, the adhesion between the film and the silicon substrate increased with increasing clay content.

The authors thank Mana Sriyudthsak and Kwanchai Anothainart from the Department of Electrical Engineering, Chulalongkorn University, for their help with the resistivity measurements.

References

1. Yano, K.; Usuki, A.; Okada, A.; Kurauchi, T.; Kamigaito, O. J Polym Sci Part A: Polym Chem 1993, 31, 2493.
2. Yano, K.; Usuki, A.; Okada, A. J Polym Sci Part A: Polym Chem 1997, 35, 2289.
3. Numata, S.; Oohara, S.; Fujisaki, K.; Imaizumi, J.; Kinjo, N. J Appl Polym Sci 1986, 31, 101.
4. Ree, M.; Goh, W. H.; Kim, Y. Polym Bull 1995, 35, 215.
5. Thompson, C.; Saraf, R. F.; Jordan-Sweet, J. L. Langmuir 1997, 13, 7135.
6. Beck Tan, N. C.; Wu, W. L.; Wallace, W. E.; Davis, G. T. J Polym Sci Part B: Polym Phys 1998, 36, 155.
7. Pinnavaia, T. J.; Lan, T.; Wang, Z.; Shi, H.; Kaviratna, P. D. In Nanotechnology: Molecularly Designed Materials; Chow, G.-M.; Gonsalves, K. E., Eds.; ACS Symposium Series 622; American Chemical Society: Washington, DC, 1996; p 250.
8. Zhu, Z.-K.; Yang, Y.; Yin, J.; Wang, X.-Y.; Ke, Y.-C.; Qi, Z.-N. J Appl Polym Sci 1999, 73, 2063.
9. Yang, Y.; Zhu, Z.-K.; Yin, J.; Wang, X.-Y.; Qi, Z.-N. Polymer 1999, 40, 4407.
10. Lan, T.; Kaviratna, P. D.; Pinnavaia, T. J. Chem Mater 1994, 6, 573.
11. Magaraphan, R.; Lilayuthalert, W.; Sirivat, A.; Schwank, J. Compos Sci Technol 2001, 61, 1253.
12. Li, W. S.; Shen, Z. X.; Zheng, J. Z.; Tang, S. H. Appl Spectrosc 1998, 52, 985.
13. Giannelis, E. P. Adv Mater 1996, 8, 3304.
14. Ghosh, M. K.; Mittal, K. L. Polyimides; Marcel Dekker: New York, 1996.
15. Ku, C. C.; Liepins, R. Electrical Properties of Polymers: Chemical Principles; Hanser Gardner: Munich, Switzerland, 1988.